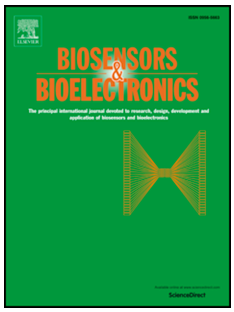

Biosensing and electrochemical properties of flavin adenine dinucleotide (FAD)-Dependent glucose dehydrogenase (GDH) fused to a gold binding peptide

Hyeryeong Lee, Yoo Seok Lee, Stacy Simai Reginald, Seungwoo Baek, Eun Mi Lee, In-Geol Choi, In Seop Chang

PII: S0956-5663(20)30421-8

DOI: https://doi.org/10.1016/j.bios.2020.112427

Reference: BIOS 112427

To appear in: *Biosensors and Bioelectronics*

Received Date: 2 June 2020

Revised Date: 29 June 2020

Accepted Date: 2 July 2020

Please cite this article as: Lee, H., Lee, Y.S., Reginald, S.S., Baek, S., Lee, E.M., Choi, I.-G., Chang, I.S., Biosensing and electrochemical properties of flavin adenine dinucleotide (FAD)-Dependent glucose dehydrogenase (GDH) fused to a gold binding peptide, *Biosensors and Bioelectronics* (2020), doi: https://doi.org/10.1016/j.bios.2020.112427.

CRediT Author Statements

- **Hyeryeong Lee**: Conceptualization, Methodology, Formal analysis, Investigation, Data Curation, Writing - Original Draft, Writing - Review & Editing, Visualization

- **Yoo Seok Lee**: Conceptualization, Writing - Review & Editing

- **Stacy Simai Reginald**: Writing - Review & Editing

- **Seungwoo Baek**: Resources

- **Eun Mi Lee**: Experimental assistance

- **In-Geol Choi**: Supervision

- **In Seop Chang**: Supervision, Project administration, Funding acquisition

Biosensing and Electrochemical Properties of Flavin Adenine Dinucleotide (FAD)-Dependent Glucose Dehydrogenase (GDH) Fused to a Gold Binding Peptide

Hyeryeong Lee [‡a], Yoo Seok Lee [‡§a], Stacy Simai Reginald [a], Seungwoo Baek [b], Eun Mi Lee [a], In-Geol Choi [b], and In Seop Chang [a]*

[a] School of Earth Sciences and Environmental Engineering, Gwangju Institute of Science and Technology, 261 Cheomdan-gwagiro, Buk-gu, Gwangju 61005, Republic of Korea

[b] Department of Biotechnology, College of Life Sciences and Biotechnology, Korea University, 145 Anam-ro, Seongbuk-gu, Seoul 02841, Republic of Korea

*Corresponding Author

E-mail: ischang@gist.ac.kr

Tel: +82-62-715-3278, Fax: +82-62-715-2434

§Present address: Department of Chemistry, University of Utah, Salt Lake City, UT 84112, U.S.A.

‡These authors contributed equally to this work

Abstract

In the present work, direct electron transfer (DET) based biosensing system for the determination of glucose has been fabricated by utilizing gold binding peptide (GBP) fused flavin adenine dinucleotide-dependent glucose dehydrogenase (FAD-GDH) from *Burkholderia cepacia*. The GBP fused FAD-GDH was immobilized on the working electrode surface of screen-printed electrode (SPE) which consists of gold working electrode, a silver pseudo-reference electrode and a platinum counter electrode, to develop the biosensing system with compact design and favorable sensing ability. The bioelectrochemical and mechanical properties of GBP fused FAD-GDH (GDH-GBP) immobilized SPE (GDH-GBP/Au) were investigated. Here, the binding affinity of GDH-GBP on Au surface, was highly increased after fusion of gold binding peptide and its uniform monolayer was formed on Au surface. In the cyclic voltammetry (CV), GDH-GBP/Au displayed significantly high oxidative peak currents corresponding to glucose oxidation which is almost c.a. 10-fold enhanced value compared with that from native GDH immobilized SPE (GDH/Au). As well, GDH-GBP/Au has shown 92.37% of current retention after successive potential scans. In the chronoamperometry, its steady-state catalytic current was monitored in various conditions. The dynamic range of GDH-GBP/Au was shown to be 3-30 mM at 30°C and exhibits high selectivity toward glucose in whole human blood. Additionally, temperature dependency of GDH-GBP/Au on DET capability was also investigated at 30-70 °C. Considering this efficient and stable glucose sensing with simple and easy sensor fabrication, GDH-GBP based sensing platform can provide new insight for future biosensor in research fields that rely on DET.

Keywords: biosensor; gold binding peptide; glucose dehydrogenase; screen-printed electrode; direct electron transfer

1. Introduction

Remarkable progress has been made in the development of biosensor and bioelectrochemical systems to obtain (1) excellent selectivity with low contributions from interfering reactions (Ispas *et al*., 2012; Wang, 2008), (2) highly efficient electrical communication of enzyme with the electrode, even over small reaction areas (Holland *et al*., 2011; Milton and Minteer, 2017; Lee *et al*., 2018; Lee *et al*., 2019), (3) small and compactly designed sensor systems that can be installed easily (Urban *et al*., 1991; Urban *et al*., 1992), and (4) minimal background ohmic resistance. There have been many efforts to satisfy those four required conditions for biosensor performance, focusing on electron transfer mechanism, biosensor design, and measurement techniques. Although there have recently been significant advances in impedimetric enzyme sensor, most of the cases are based on amperomeric enzyme sensor and three generations have been reported depending on electron acceptors (Ito *et al*., 2019). In particular, 3rd-generation biosensor employing the direct electron transfer (DET) principle, has been considered to be fascinating since it functions without artificial electron mediator that is toxic chemical and could possibly cause unnecessary side-reactions in complex physiological environments (Léger and Bertrand, 2008).

To date, several studies have reported for DET capable enzyme-electrode using various immobilization method. In the previous study from Ishida *et al.* (2018), FAD-GDH from *Aspergillus flavus* was adsorbed on the single-walled carbon nanotube layer for effective electrical contact of enzymatic cofactor and electrode surface (Ishida *et al*., 2018). From Ito *et al.* (2019), electron transfer domain of cellobiose dehydrogenase (CDH), heme *b*-binding cytochrome domain, was genetically fused to *Aspergillus flavus* derived FAD-GDH to induce a flavin-to-heme interdomain electron transfer. Thereby, non-DET type FAD-GDH has granted DET capability by the support of additional electron transfer protein (Ito *et al*., 2019). The direct conjugation of mediating molecules such as quinone derivatives, various osmium-complexes, ferrocene derivatives, etc. was also shown to provide redox potentials appropriate for pulling electrons from the cofactor to the electrode (Babanova *et al*., 2014; Babanova *et al*., 2015). Additionally, gold nanoparticles and cytochrome *c* have been incorporated to facilitate electron transfer across enzyme–electrode interfaces (Ratautas *et al*., 2016; Algov *et al*., 2017). To optimize the DET at the enzyme-electrode interface, however, the final electron donor in electroactive enzymes (e.g. FAD, metallocofactor, etc.) should be controlled to face toward electrode surface and to be in close proximity with it. If

the orientation of enzymes in working electrode of enzyme-based electrochemical sensor is not properly regulated, applied potential in biosensing device would shift in positive direction, increasing the chance of oxidoreduction of co-present interferent molecules with target analyte and decreasing sensing accuracy.

To regulate the enzyme orientation for enzymatic cofactor to face toward electrode surface, the enzyme-electrode linking method and fusion site in enzyme should be considered as highly important factors. Improper linkage of amino acid could possibly occur the conformational change of enzymes following with loss of enzyme activity or widen the inter-distance between enzymatic active site and electrode surface. In the previous study, substrate-like compound (e.g. anthracene-2-diazonium, 4-azidoaniline, etc.) that interacts with the redox site of the enzyme as ligand was covalently functionalized on the electrode surface, thereby inducing a preferential orientation of the enzymatic active site towards the electrode (Martinez-Ortiz *et al*., 2011; Arrocha *et al*., 2014). Although there have been many linkage methods suggested for DET at enzyme-electrode interface, however, it is still hard to precisely control the enzyme orientation in single molecule level.

To overcome these hurdles, we recently reported an efficient approach for DET-capable enzyme *via* genetic expression of a gold binding peptide (GBP) comprising 12 amino acids (LKAHLPPSRLPS, 1.3 kDa) that form a sticky end with a specific binding affinity (microelectronic and magnetic affinity) toward a surface of specific metal. As the fusion site of GBP is the important parameter that determines the enzyme binding orientation as well as proximity of cofactor with electrode surface, the GBP has expressed C- or N-terminus of enzyme subunits and DET efficiency at each modified structures was compared and analyzed (Lee *et al*., 2018; Lee *et al*., 2019).

The FAD-dependent glucose dehydrogenase (FAD-GDH) from *Burkholderia cepacia* which has been chosen as model enzyme is a thermostable, oxygen-independent and DET capable enzyme. This enzymatic property makes FAD-GDH practical which can be applied in various temperature. The FAD-GDH is made up of three subunits; catalytic subunit (α-subunit) containing FAD as an active site; electron transfer subunit (β-subunit) in which heme-containing cytochrome *c* is present; and small subunit (γ-subunit) that is a firming unit for α- and β-subunits (Arrocha *et al*., 2014). The entire FAD-GDH complex displayed DET with a relatively low bioelectrocatalytic current and a redox potential of –460 mV (*vs.* Ag/AgCl) at pH 7.0. The size of the β subunit, which enabled electron transfer in the native GDH, as well as the random orientations of the enzyme, reduced the efficiency of electron

transfer to the electrodes. Algov *et al.* (2017) has proven that the large proteinaceous matrix of *β*-subunit in FAD-GDH introduces additional insulation during interfacial electron transfer and increases charge transfer resistance for interfacial electron transfer, reducing electron transfer efficiency. They have shown that the omission of *β* subunit in FAD-GDH is beneficial for enhancing enzymatic activity for glucose oxidation as well as direct electrocatalytic activity of enzyme-electrode *via* shortening electron transfer distance (Algov *et al*., 2017). Another previous study from Okuda-Shimazaki *et al*. (2008) has proven that the expression of *α*-subunit of FAD-GDH alone could retain almost 100% of catalytic current on electrode after 24-hour operation as well as bioactivity. Meanwhile, it was also shown that the *β* subunit exhibits the lowest stability among the three subunits of FAD-GDH (Inose *et al*., 2003). Therefore, a site-specific attachment of gold-binding peptide near the active center of the *α* subunit and the omission of the *β* subunit in FAD-GDH complex is assumed to reduce the number of electron transfer intermediates as well as shortening the electron transfer distance, achieving an efficient DET-based biosensor (Lee *et al*., 2018).

In this study, GBP-fused FAD-GDH (GDH-GBP) derived from *Burkholderia cepacia* was applied on screen-printed electrode (SPE), producing GDH-GBP immobilized SPE (GDH-GBP/Au). We have attempted to fabricate upgraded biosensor with enzymatic orientation controllability, DET capability and simplicity in enzyme immobilization on a compactly designed sensor system without chemical supports. We have compared electrochemical and mechanical activity of GDH-GBP with those of native GDH on electrode. Their binding affinities on Au substrate were analyzed by Quartz crystal microbalance (QCM). The binding morphology of enzymes on Au electrode were imaged by atomic force microscopy (AFM). Most importantly, the biosensing property of GDH-GBP/Au was electrochemically investigated using cyclic voltammetry and chronoamperometry. As well, GDH-GBP/Au was tested to measure glucose contents in human whole blood samples and the result was compared with conventional blood sugar assessment method to evaluate biosensor applicability in clinical diagnostics. Furthermore, the effects of temperature on the DET efficiency of biosensor was also estimated under 30-70°C.

2. Materials and methods

2.1. Enzyme Preparation.

Synthetic constructs that comprises GDH α-subunit with GBP (LKAHLPPSRLPS, 1.3 kDa) at C-terminus and GDH γ-subunit with GBP at N-terminus were cloned into modified pET21a plasmid and transformed to *E. coli* BL21 - CodonPlus (DE3) - RIL (Agilent Technologies, USA). The *E. coli* BL21(DE3) were then cultivated, and the synthetic GDH was expressed and purified. The SDS page analysis has been reported in previous work (Lee *et al*., 2018; Lee *et al*., 2019).

2.2. AFM Characterization

High-resolution atomic force microscopy (AFM) was used to visualize the surface of an enzyme film on the electrode surface. Prior to AFM characterization, gold-coated silicon wafer (cut by 1 cm × 1 cm) was cleaned by being immersed in piranha solution (3:1 v/v, H_2SO_4:H_2O_2) for 10 min to remove inorganic and organic contaminants from the gold surface. Then, the Au electrode was fully incubated in 0.5 μM of native GDH and GDH-GBP solution in phosphate buffer (pH 7.0) for 120 min with stirring, to immobilize target proteins on gold substrate. After incubation of gold substrate in protein solution, the unbound and weakly bound enzymes were thoroughly washed away in a stream of deionized water and blow-dried with air. AFM measurements were obtained in the non-contact mode using an XEP system controller (AFM, XE-200, PSIA Corporation) (Okuda-Shimazaki *et al*., 2008).

2.3. Quartz Crystal Microbalance (QCM) Characterization

The binding affinities of the native GDH and GDH-GBP on the gold electrodes were measured using a quartz crystal microbalance (QCM; SEIKO EG & G, Ltd., Japan). The change in resonance frequency of piezo-electric quartz chip is monitored during adsorption of proteins. The frequency is typically proportional to the protein mass on the electrode. Thus, the enzyme solution containing the native GDH and GDH-GBP were dropped onto the gold-coated QCM electrode. The frequency was then monitored using the WinQCM software for 120 min (Okuda-Shimazaki *et al*., 2008; Kacar *et al*., 2009).

2.4. Enzyme Immobilization on Screen-printed Electrode

Screen-printed electrode (SPE) was purchased from DropSens (Spain). The SPE is in three-electrode cell configuration printed on ceramic substrates (dimensions: 3.4 × 1.0 × 0.05 cm; length × width × height). The working (disk-shaped 4 mm diameter) and counter

electrodes were made of gold ink and platinum ink, respectively. The pseudoreference electrode and the electric contacts were formed from silver. For the immobilization of enzymes, native GDH or GDH-GBP, an aliquot of enzyme solution (5μM, 30 μL) containing native GDH or GDH-GBP was dropped onto the working electrode surface of the SPE and allowed to incubate for 120 min. The enzyme solution on the SPE was gently resuspended by pipetting every 30 min. Then, the SPE was fully washed with phosphate buffer (pH 7.0) to remove weakly bound enzyme remained on the gold surface. The enzyme immobilized SPEs were installed in reactors with a working volume of 8 mL and were connected to a potentiostat (Metrohm AutoLab, Utrecht, Netherlands) through the specific DropSens connector (Spain) present in each case.

2.5. Electrochemical Measurements

The CV and chronoamperometry of fabricated biosensors were performed using a potentiostat (Metrohm AutoLab) in a PBS (100 mM, pH 7.0) buffer containing 100 mM glucose. The electrochemical properties were characterized using CV conducted over the potential range –800 mV to 600 mV (*vs.* Ag/Ag^{+}), at a scan rate of 50 mV s^{-1} unless otherwise indicated. Chronoamperometry was tested by applying a continuous –200 mV potential to the working electrode up to 10 min. At the initial state of detection, the transient background currents were allowed to decay to a steady-state value and the steady-state current was recorded as result of the electrocatalytic oxidation of glucose.

2.6. Determination of Glucose Contents in the Blood Samples.

The fabricated glucose biosensor, GDH-GBP/Au, was used to determine the glucose concentration of the blood samples. Whole blood samples (5 samples) were obtained from National Biobank of Kyungpook National University Hospital (Daegu, Korea). The results of blood glucose concentration from the biosensor were compared with that from glucose assay kit (GAHK20; Sigma Chemical Co.). Prior to measurement of glucose contents using glucose assay kit, the blood serum was extracted after centrifugation of whole blood. The analysis was conducted in duplicate using UV–VIS spectrophotometer (V-730, Jasco, Japan) at 340 nm.

3. Results and discussion

3.1. Electrochemical properties of the native- and GBP-fused FAD-GDHs on Au electrode

The native GDH and GDH-GBP immobilized electrodes were characterized using CV to confirm electrochemical properties. From the Fig. 1, The anodic current of GDH-GBP/Au started to be significantly increased from –455 mV (*vs.* Ag/AgCl) while the that of native GDH immobilized SPE (GDH/Au) started to appear from ~0.0 V, with relatively low electrocatalytic response. The CV result of GDH-GBP/Au provided evidence for DET between the FAD center and the electrode, based on the information that FAD/$FADH_2$ has a formal potential ($E^{0'}$) of –460 mV (*vs.* Ag/AgCl) at pH 7.0 (Holland *et al*., 2011). These observations proved that GDH-GBP could transfer the electrons without electron transfer subunit and chemical supports on electrode.

As the peak currents in Fig. 1 of the both enzyme-electrodes are compared, oxidative peak current of GDH-GBP/Au, at c.a. -0.25 V, was almost 10 times enhanced in response to enzyme-catalyzed glucose oxidation compared to GDH/Au. Thereby, the fusion of GBP to specific site of FAD-GDH has shown to led dramatic increase in anodic current of FAD-GDH based SPE. It was also observed that the large catalytic current of GDH-GBP/Au is attributed to the glucose oxidation during comparison analysis in the presence or absence of glucose (Fig. S1). Since FAD-GDH could oxidize only D-glucose, the reactions occurring in the enzyme-electrode, GDH/Au and GDH-GBP/Au both can be summarized as:

$$\mathrm{D-glucose} + \mathrm{FAD\text{-}GDH}_{ox} \rightarrow \mathrm{D-glucono-1{,}5-lactone} + \mathrm{FAD\text{-}GDH}_{red} \quad (1)$$

$$\mathrm{FAD\text{-}GDH}_{red} \rightarrow \mathrm{FAD\text{-}GDH}_{ox} + 2e^{-} \quad (2)$$

where the subscripts ox and red refer to oxidized and reduced forms, respectively.

However, unexpected oxidation peaks were appeared at 0.0 to 0.2 V (*vs.* Ag/AgCl, Fig. 1A) from GDH-GBP/Au. These peaks could be reasoned that enzyme is immobilized on the electrode under the thermodynamically and kinetically unfavorable condition for direct electric communications (Lee *et al*., 2019). Inefficient orientation of enzymes partially exists on the electrode, causing the potential shifts to be more positive potential compared with enzymes well oriented on the electrode.

Catalytic current stability was measured by monitoring the response after continuous potential scans of the GDH-GBP/Au. As shown in Fig. 1A, the current response at the GDH-GBP/Au has shown little change after 20 cycles, retaining almost 92.37% of the initial catalytic current when comparing initial and final peak current (i_p) in cyclic voltammogram (Table S1). These observations corroborated that over a moderate sensing operation time (seconds to minutes), the electron transfer conditions in the GDH-GBP/Au device is favorable for stable maintenance of electrocatalytic current at the enzyme-electrode interface.

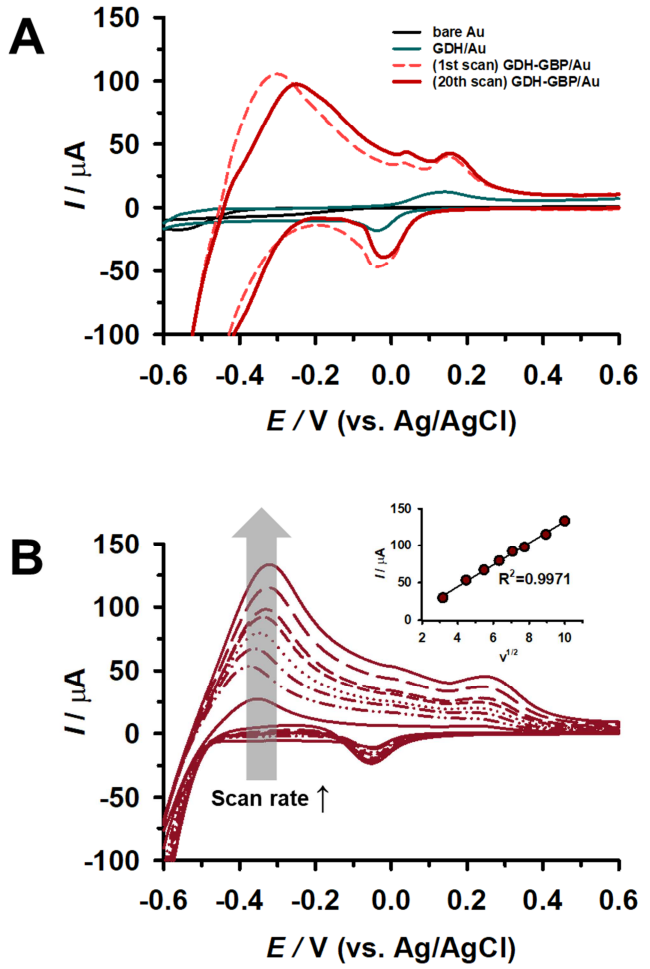

Fig. 1. (A) CV profiles of a bare Au electrode, GDH/Au, 1st and 20th scans of GDH-GBP/Au in the presence of 100 mM glucose in a PBS buffer (100 mM, pH 7.0). (B) Dependence of the electron transfer of GDH-GBP/Au on the scan rate (100, 80, 60, 50, 40, 30, 20, and 10 mV s^{-1}) (inset: dependence of the peak current on root square of the scan rate).

3.2. Au binding kinetics and morphological characterization of the FAD-GDHs on Au substrate

The binding kinetics of the native GDH and GDH-GBP proteins bound to the Au electrode surfaces were characterized using a quartz crystal microbalance (QCM, Fig. 2A) (Okuda-Shimazaki *et al*., 2008). As the incubation time of the enzyme solution lengthened, the GDH-GBP presented a steep increase in the frequency change compared with the native protein. It was shown that GDH-GBP provided a much higher gold binding activity than the native GDH, as expected. This result is corresponding to surface plasmon resonance (SPR) spectroscopy results provided in the previous work (Lee *et al*., 2018).

Topographical information of the native GDH and GDH-GBP on Au surface was collected using high-resolution AFM (Fig. 2B). The GDH-GBP was found to be tightly packed and regularly distributed across the electrode surface, whereas the native GDH formed a more irregular film. The height of native GDH layer (8.53 ± 5.62 nm) on Au surface was higher with a larger standard deviation than that of the GDH-GBP (6.89 ± 1.97 nm) layer, indicating that the native GDH tended to form multi-stacked enzyme layers, possibly due to enzymatic agglomeration along the direction perpendicular to the surface. Furthermore, the GDH-GBP formed a packed and uniform monolayer which thickness is very close to the size of a single molecule of FAD-GDH (~6 nm), suggesting that the GBP unit strongly bound and positioned to Au surface in a uniform manner and enabled the catalytic subunit of GDH-GBP to face the electrode surface (Okuda-Shimazaki *et al*., 2008; Lee *et al*., 2018). Taken together, these findings indicated that fusion of GBP to enzyme could be able to control enzymatic orientation as well as binding uniformity on the electrode surface, which is importantly required DET-based enzyme electrode.

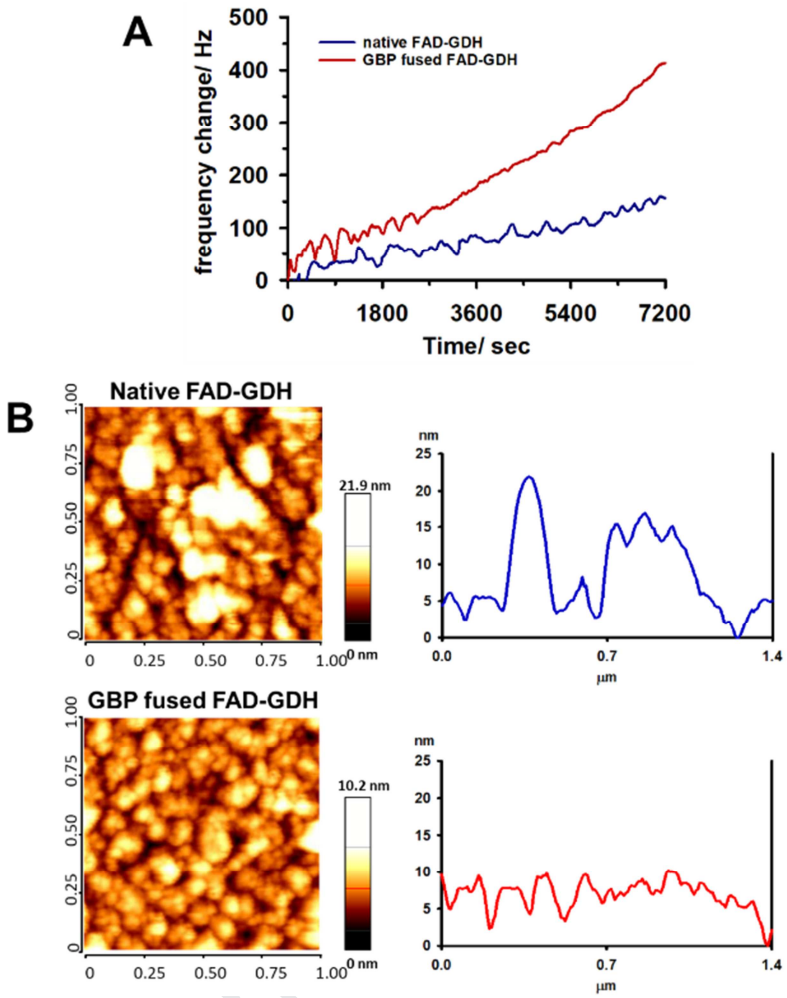

Fig. 2. Gold binding characteristics of the native- and GBP-fused FAD-GDH. (A) Gold binding activities of the native- and GBP-fused FAD-GDH on a gold-coated quartz crystal, determined by measuring the frequency changes using quartz crystal microbalance (QCM) analysis. (B) AFM images showing the surface topographies of the native- and GBP-fused FAD-GDH system (protein concentration: 55 μg mL^{-1}). The areas correspond to 1 μm × 1 μm scans.

3.3. Amperometric response of GBP-fused FAD-GDH on screen-printed Au electrodes as a function of glucose concentration

To evaluate the biosensor performance, the steady-state amperometric response of the GDH-GBP was measured on a compactly designed screen-printed Au electrode (Fig. 3). The biosensor exhibited a rapid and sensitive response to the addition of glucose. The current for GDH-GBP/Au increased after the injection of glucose and achieved 95% of the steady-stated current in 5–30 s. The current was found to increase with increasing glucose concentration, with a dynamic range from 3 to 30 mM (correlation coefficient, R^2 = 0.9918). The sensitivity in the linear region was determined by linear regression analysis up to

30 mM. The linear regression equation could be expressed as: I (μA) = 1.33C - 1.71 (mM). The GDH-GBP/Au yielded a sensitivity of 1.33 μA mM^{-1} cm^{-2} and a detection limit of 3.41 mM (based on a signal-to-noise (S/N) of 3). The GDH-GBP/Au showed exceptional sensitivity and a low detection limit compared to the DET-based biosensor. These results indicated reliable electrocatalytic oxidation and fast enough electron exchange in the biosensor due to fuel oxidation at a low redox potential, without interference from background redox mediators (*i.e.*, thermodynamic losses resulting from a negative change in the Gibbs free energy).

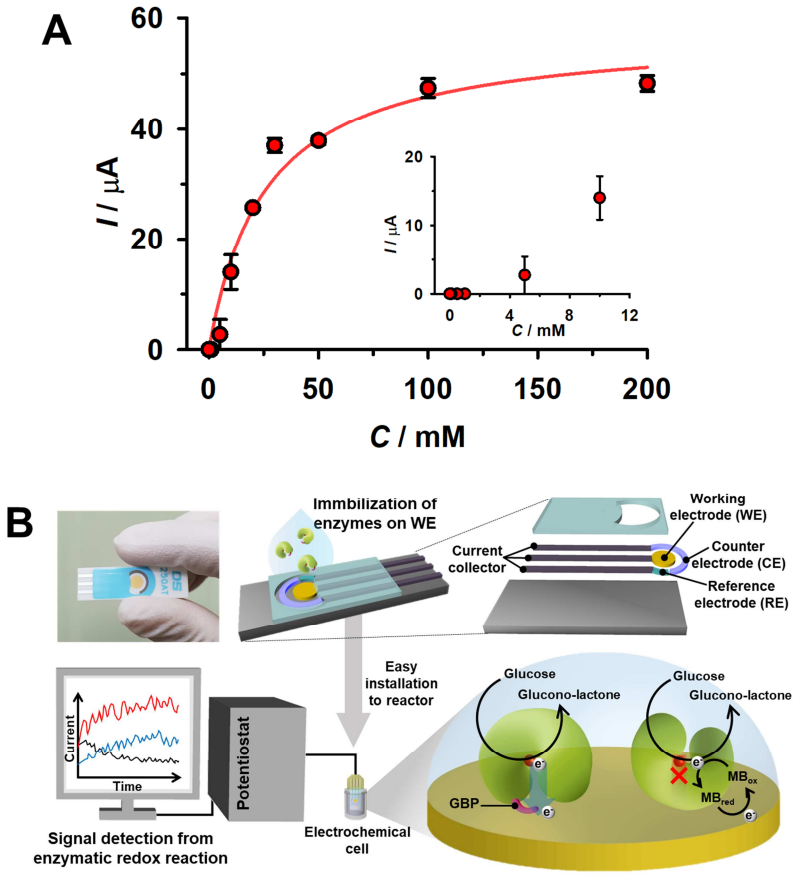

Fig. 3. (A) Dependence of the steady-state catalytic current at the GDH-GBP/Au on the 0 to 200 mM of glucose concentration. (Insert: Dotted trace represents the current response up to 10 mM of glucose concentration) Data fitted to the Michaelis-Menten equation by using non-linear regression analysis. (B) Schematic illustrations of the screen-printed electrode used here, the electrochemical characterization of the enzyme–electrode, and interfacial electron transfer of native- and GBP-fused FAD-GDH on surface of the screen-printed electrode (top inset: photograph of a bare screen-printed electrode).

For the kinetic analyses of the GDH-GBP immobilized on gold surface, data were fitted to a Michaelis-Menten type equation and the maximum steady-state current response (i_{max}) and apparent Michaelis-Menten constant (K_M^{app}) for glucose were determined. Data was fitted to the Michaelis–Menten equation by using non-linear regression analysis with Sigmaplot 14.0;

$$1/i = (K_M^{app}/i_{max})(1/C) + 1/i_{max} \quad (3)$$

where C is the concentration of glucose, i is the measured current at each glucose concentration, and i_{max} is the saturation value of the current. Here, K_M^{app} reflected the bioactivity and affinity toward glucose of FAD-GDH on electrode.

According to the non-linear regression analysis, the K_M^{app} was calculated to be 26.91±4.31 mM, much lower than that of many other matrices (Fig. 3B). The low K_M^{app} indicated good bioactivity among the immobilized GDH molecules was preserved. Based on the calculated i_{max}, furthermore, the electron transfer efficiency (η_{ET}) (%) was calculated to examine the quality of developed GDH-GBP/Au in the term of percentage ratio of electroactive enzymes to surface occupied enzymes. This term refers to the ratio of the number of generated electrons from enzymatic redox reaction to the number of electrons collected by electrode and thus indicates the percentages of electroactive enzymes which practically works to transfer electrons toward electron accepter, electrode (scheme S1). This approach to evaluate the biosensor could be helpful to accurately compare obt0061ined performance from this work with others, regardless of quantitative current level, enzyme mass used, electrode size, etc. The electron transfer efficiency of GDH-GBP/Au was calculated using following equation (Vazquez‐Duhalt *et al*., 2014; Kim *et al*., 2016; Lee *et al*., 2018).:

$$\eta_{ET}\ (\%) = \frac{(Measured\ current)}{(Theoretical\ current)} \times 100 = \frac{(Measured\ Current)}{(\text{Specific activity} \times \text{Enzyme mass} \times n \times \text{Faraday constant})} \times 100 \quad (4)$$

Here, it should be noted that the term, electron transfer efficiency (η_{ET}) indicates the ratio of transferred electron number from enzymatic cofactor toward electrode *vs.* the number of electrons that could be generated from enzymatic cofactor based on specific activity of FAD-GDH. The specific activity of enzyme was measured using the DCIP method reported in the previous study (Lee *et al*., 2018). The electron transfer efficiency was calculated *via* ratio of

353 theoretical current (μA) and actual measured current (μA) at the enzyme-electrode. The i_{max} in
354 Michaelis-Menten models was used as measured current term. The theoretical current was
355 obtained using the specific activity (μmol min^{-1} mg^{-1}) of enzyme, the enzyme mass (μg) used,
356 and number of electrons involved in the enzymatic reaction, *n*. The obtained electron transfer
357 efficiency of GDH-GBP/Au was measured to be 6.54±0.18% at 30°C. The obtained electron
358 transfer efficiency from GDH-GBP/Au is orders of magnitude higher than previously
359 reported DET based enzyme-electrode system.

360 Biosensor selectivity, which indicates the ability to discriminate the interfering species
361 from the target analyte, is an important factor for amperometric biosensor. Amperometric
362 detection of glucose using enzyme-based biosensor is generally interfered by other sugars,
363 such as galactose, fructose, xylose, etc. and reducing compound such as ascorbic acid, uric
364 acid, acetaminophen, etc. those could be present in physiological condition. An interference
365 test was carried out by injecting the potential interfering species, other sugars including
366 galactose, fructose, xylose and reducing compound including ascorbic acid, uric acid, and
367 acetaminophen. The two types of interfering substances which are other sugars and reducing
368 compounds were separately tested (Fig. 4). It was shown that the additions of each
369 interfering substance did not substantially change the response signal and the initial
370 amperometric signal for glucose detection was almost retained, indicating excellent
371 selectivity of the biosensor toward glucose detection.
372

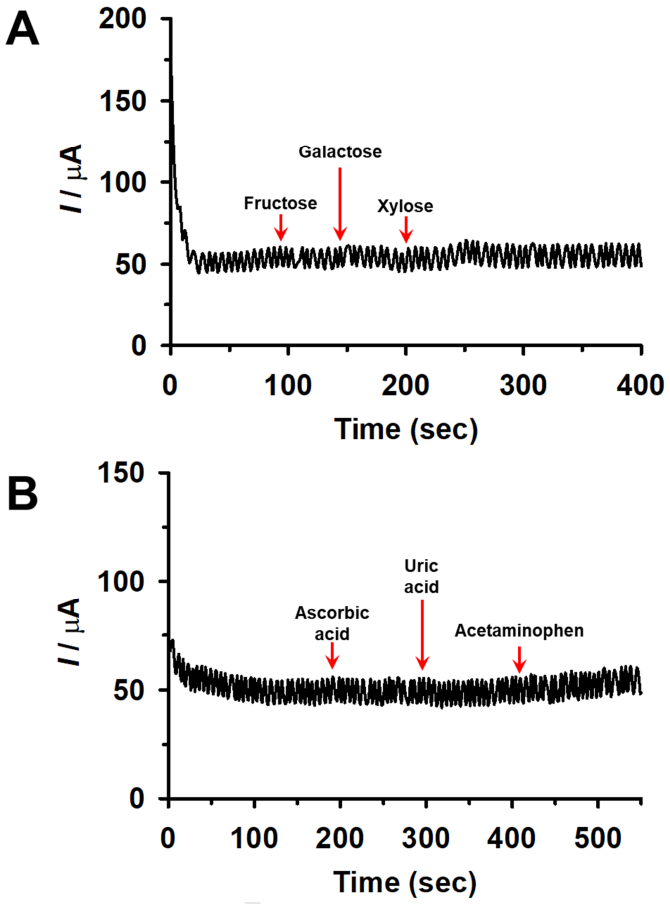

Fig. 4. Amperometric response of GDH-GBP/Au to sequential addition of (A) 10 mM of other type sugars (fructose, galactose, and xylose) and (B) 1 mM of reducing compounds (ascorbic acid, uric acid, and acetaminophen) in PBS solution after initial addition of 100 mM of glucose at an applied potential of -0.2 V (*vs.* Ag/AgCl)

The storage stability of biosensor for long-term period was evaluated *via* measuring the amperometic response after 43 days of storage of biosensor. When not in use, the biosensor was stored at 4°C in a refrigerator, after initial electrochemical test. The results are shown in Fig. S2. After 43 days of initial operation of biosensor, the response retained over 82% of the initial value. The high stability of the DET-based GDH-GBP/Au was attributed to the gold binding peptide, which provided a strong and stable binding of FAD-GDH on the electrode. In addition, the genetic engineering of FAD-GDH, which expressed GBP on the catalytic subunit of GDH, preserved the bioactivity of the native GDH and played an important role in the catalytic stability of the enzymes in the biosensor.

Then, The GDH-GBP was tested with human whole blood samples for evaluating its applicability in clinical diagnostics (Heller and Feldman, 2008; González-Gaitán *et al.*, 2017). Five whole blood samples were used to determine glucose concentration in human whole

391 blood. Each sample was measured with two different detection protocols in duplicate (Table
392 S2 and S3). The blood sugar contents measured with biosensor was compared with those
393 measured with conventional method using glucose assay kit (Table 1). In comparison of
394 conventional method, the relative errors were shown to be less than 10%, which indicates the
395 developed GDH-GBP/Au could be potentially used for the detection of clinical blood
396 samples.
397
398 **Table 1.** Assessment of blood sugar content using GDH-GBP/Au based biosensing system and
399 conventional method.

Number of whole blood samples	Glucose concentration measured by HK protocols (mM) (a)	Glucose concentration measured by GDH-GBP/Au based biosensor (mM) (b)	Relative deviation (%)[a]
1	6.68±0.01	8.17±0.36	9.19
2	5.57±0.03	6.39±0.07	3.97
3	5.30±0.01	6.35±0.08	8.11
4	5.07±0.00	5.72±0.17	4.64
5	4.72±0.01	5.22±0.22	6.49

400 [a]Relative deviation (%) = 100×|b-a|/b (The average value was used for calculation of relative
401 deviation.)
402
403 **3.4. Operating temperature effects on biosensing properties**

404 Operating temperature is one of the parameters that affects the function of enzymes. The
405 FAD-GDH used in this work was derived from a thermophilic strain, *Burkholderia cepacia*,
406 and showed a range of specific activities toward glucose oxidation at temperatures from 30
407 to 70°C (Martinez-Ortiz *et al*., 2011; Gineitytė *et al*., 2019). The temperature-dependent DET
408 kinetics and thermodynamics of GDH-GBP/Au and were primarily investigated using CV at
409 temperatures of 30-70°C. Together with CV measurement, the specific activity of the free
410 GDH-GBP was measured to analyze how the temperature change affects DET efficiency of
411 GDH-GBP/Au. The specific activity of the GDH-GBP was shown to remain nearly constant
412 over the range 30-50°C and dramatically decreased at temperatures of 60–70°C (Fig. S4).
413 Interestingly, the CV results showed that GDH-GBP/Au provided a peak current that
414 increased significantly within the range 30-50°C, while the specific activity of the free
415 GDH-GBP is almost retained at the same temperature range. In the temperature dependent

cyclic voltammogram of GDH/Au, almost no change in anodic curve was observed, indicating that temperature dependent change in peak current of GDH-GBP/Au has occurred due to transition at the enzymatic cofactor-electrode (Fig. S5). The DET kinetics at the enzyme–electrode interface is mainly determined by the enzyme catalytic activity and interfacial electron delivery, which is strongly dependent on the proximity of the cofactor with the electrode surface. Since the generated electrons are constant at 30-50°C as the specific activity was shown not to change, elevated the DET kinetics at 30-50°C might mainly due to the enzyme structural folding on the electrode surface, affecting interfacial distance between cofactor and electrode surface. At 60–70°C, the catalytic current of GDH-GBP/Au was shown to be declined and this is assumed that the DET kinetic was mainly dependent by reduced turnover rate of GDH-GBP. In addition, the onset potential of GDH-GBP/Au at 30–70°C was shifted toward less positive values, regardless of the electron transfer kinetics. This negative shifts in the onset and peak potentials was ascribed to Nernstian behavior. These results show that the DET efficiency was mainly governed by the interfacial environment of the enzyme–electrode at 30–50°C and by the change in the specific activity at higher temperatures of 60–70°C (Fig. S4).

The temperature dependence of amperometric signal was also obtained at various glucose concentrations ranging between 0 to 200 mM. As above, the amperometric signal of GDH-GBP/Au based biosensing system at 30°C shows linearity from 3 mM to 30 mM glucose. As incubation temperature of the system increases, its dynamic range has extended with decreased low limit (up to 0.5 mM) and increased upper limit of linear detection range (up to 50 mM). Here, the K_M^{app}, which is related to the substrate binding affinity of immobilized GDH-GBP on the electrode was calculated with non-linear regression analysis from the amperometric results shown in Fig. 5A. The electrochemical K_M^{app} values of GDH-GBP/Au at 30, 40, 50°C were calculated to be 26.91±4.31, 23.92±3.07, and 22.32±3.07 mM, respectively, and remained relatively unchanged at 30–50°C. The temperature dependence of the electrochemical K_M^{app}, was similar with result in specific activity of the free GDH-GBP. However, the i_{max} values increased dramatically with the incubation temperature: 58.29±1.62, 76.00±1.21, and 103.53±10.17 μA at 30, 40, 50°C, respectively (Fig. 5 and Table S2).

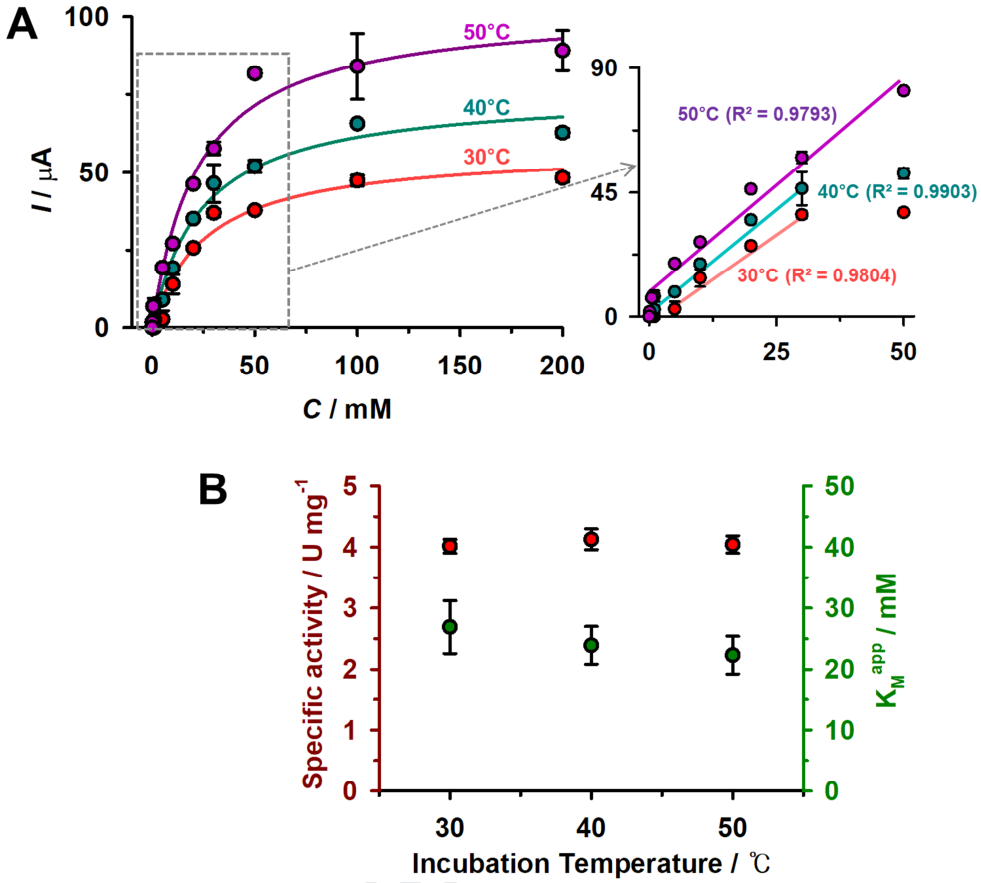

Fig. 5. (A) Dependence of the steady-state catalytic current at the GDH-GBP/Au on the glucose concentration (0 to 200 mM) at different incubation temperatures (30, 40, and 50°C). Applied potential is -0.2 V (*vs.* Ag/AgCl) Data fitted to the Michaelis-Menten equation by using non-linear regression analysis. (B) Plot of K_M^{app} of GDH-GBP/Au obtained from the glucose concentration-dependent amperometric signals (green) and the specific activity of the free GBP-fused FAD-GDH of the electrolyte at 30, 40, 50°C (red).

Additionally, the electron transfer efficiency of GDH-GBP/Au at each incubation temperature was calculated and compared (Table S4). Electron transfer efficiency at 30°C was shown to be 6.54±0.18%. As the incubation temperature increased gradually, the electron transfer efficiency also increased, showing 8.52±0.14% and 11.61±1.14% at 40 and 50°C. The electron transfer efficiency at 50°C, obtained from enzyme–electrode incubation, was twice the value obtained at 30°C. This result demonstrated that favorable DET kinetics at elevated incubation temperatures could be ascribed to the interfacial conditions between the enzymatic cofactor and the electrode. Considering that enzymatic activity was constant at 30-50°C in the state of both free and immobilized GDH-GBP, it could be proven that

enzyme conformational change on electrode has enabled closer contact between enzymatic cofactor and electrode surface. Here, it could be known that the temperature should be importantly considered for glucose monitoring using GDH-GBP/Au depending on its application sites.

4. Conclusion

In this study, we demonstrated a DET-based GDH-GBP/Au system, an integration of an engineered oxidoreductase and a screen-printed electroanalytical sensing platform. The GDH-GBP/Au displayed mechanical, biochemical, and electrochemical characteristics suitable for DET based biosensing applications. The GDH-GBP/Au was capable of direct transfer of electrons toward the electrode as indicated by the significant increase in the oxidative current from a response to the enzyme-catalyzed glucose oxidation. The catalytic current was highly retained, recording 92.37% of catalytic current after successive potential scans. DET-based GDH-GBP/Au system has showed high sensitivity of 1.33 μA mM^{-1} cm^{-2} within the linear range of 3 to 30 mM at 30°C and good resistance towards interfering species. In the evaluation of storage stability, current response of GDH-GBP/Au was highly retained for over one month. In the glucose determination with whole blood sample, GDH-GBP/Au has shown < 10% of the relative errors, proving its potential usage for the detection of clinical blood samples. The temperature dependency of GDH-GBP/Au has been also estimated to analyze the effect of surrounding temperature of application sites. The GDH-GBP/Au has been well operated in the temperature range of 30-50°C. Therefore, the produced GDH-GBP/Au electrode shows promise in the wide range biosensing applications. Furthermore, suggested technique could be potentially applied to different type of enzyme-based biosensors in which adopts various DET-capable (FAD, FMN, PQQ, or Moco dependent) oxidoreductases.

Acknowledgements

H. Lee and Y. S. Lee contributed equally. This work was supported by grants from the National Research Foundation of Korea (NRF), funded by the Korean Government (2020R1A2C3009210). The biospecimens and data used for this study were provided by National Biobank of Korea-Kyungpook National University Hospital(KNUH), a member of the KoreaBiobank Network-

KNUH and all biospeciments were obtained (with informed consent) under institutional review board (IRB)-approved protocols.

References

Algov, I., Grushka, J., Zarivach, R., Alfonta, L., 2017. J. Am. Chem. Soc. 139, 17217–17220.

Arrocha, A.A., Cano-Castillo, U., Aguila, S.A., Vazquez-Duhalt, R., 2014. Biosens. Bioelectron. 61, 569–574.

Babanova, S., Matanovic, I., Atanassov, P., 2014. ChemElectroChem 1, 2017–2028.

Babanova, S., Matanovic, I., Chavez, M.S., Atanassov, P., 2015. J. Am. Chem. Soc. 137, 7754–7762.

Gineitytė, J., Meškys, R., Dagys, M., Ratautas, D., 2019. J. Power Sources 441, 227163.

González-Gaitán, C., Ruiz-Rosas, R., Morallón, E., Cazorla-Amorós, D., 2017. RSC Adv. 7, 26867–26878.

Heller, A., Feldman, B., 2008. Chem. Rev. 108, 2482–2505.

Holland, J.T., Lau, C., Brozik, S., Atanassov, P., Banta, S., 2011. J. Am. Chem. Soc. 133, 19262–19265.

Inose, K., Fujikawa, M., Yamazaki, T., Kojima, K., Sode, K., 2003. Biochim. Biophys. Acta (BBA)-Proteins Proteomics 1645, 133–138.

Ishida, K., Orihara, K., Muguruma, H., Iwasa, H., Hiratsuka, A., Tsuji, K., Kishimoto, T., 2018. Anal. Sci. 34, 783–787.

Ispas, C.R., Crivat, G., Andreescu, S., 2012. Anal. Lett. 45, 168–186.

Ito, K., Okuda-Shimazaki, J., Mori, K., Kojima, K., Tsugawa, W., Ikebukuro, K., Lin, C.-E., La Belle, J., Yoshida, H., Sode, K., 2019. Biosens. Bioelectron. 123, 114–123.

Ito, Y., Okuda-Shimazaki, J., Tsugawa, W., Loew, N., Shitanda, I., Lin, C.-E., La Belle, J., Sode, K., 2019. Biosens. Bioelectron. 129, 189–197.

Kacar, T., Zin, M.T., So, C., Wilson, B., Ma, H., Gul‐Karaguler, N., Jen, A.K., Sarikaya, M., Tamerler, C., 2009. Biotechnol. Bioeng. 103, 696–705.

Kim, S., Jang, L.K., Park, H.S., Lee, J.Y., 2016. Sci. Rep. 6, 1–8.

Lee, H., Lee, Y.S., Lee, S.K., Baek, S., Choi, I.-G., Jang, J.-H., Chang, I.S., 2019. Biosens. Bioelectron. 126, 170–177.

Lee, Y.S., Baek, S., Lee, H., Reginald, S.S., Kim, Y., Kang, H., Choi, I.-G., Chang, I.S., 2018. ACS Appl. Mater. Interfaces 10, 28615–28626.

Léger, C., Bertrand, P., 2008. Chem. Rev. 108, 2379–2438.

Li, D., He, Q., Cui, Y., Duan, L., Li, J., 2007. Biochem. Biophys. Res. Commun. 355, 488–493.

Martinez-Ortiz, J., Flores, R., Vazquez-Duhalt, R., 2011. Biosens. Bioelectron. 26, 2626–2631.

Milton, R.D., Minteer, S.D., 2017. J. R. Soc. Interface 14, 20170253.

Okuda-Shimazaki, J., Kakehi, N., Yamazaki, T., Tomiyama, M., Sode, K., 2008. Biotechnol. Lett. 30, 1753–1758.

Ratautas, D., Laurynėnas, A., Dagys, M., Marcinkevičienė, L., Meškys, R., Kulys, J., 2016. Electrochim. Acta 199, 254–260.

Urban, G., Jobst, G., Kohl, F., Jachimowicz, A., Olcaytug, F., Tilado, O., Goiser, P., Nauer, G., Pittner, F., Schalkhammer, T., 1991. Biosens. Bioelectron. 6, 555–562.

Urban, G., Jobst, G., Keplinger, F., Aschauer, E., Tilado, O., Fasching, R., Kohl, F., 1992. Biosens. Bioelectron. 7, 733–739.

Vazquez‐Duhalt, R., Aguila, S.A., Arrocha, A.A., Ayala, M., 2014. ChemElectroChem 1, 496–513.

Wang, J., 2008. Chem. Rev. 108, 814–825.

Table captions

Table 1. Assessment of blood sugar content using GDH-GBP/Au based biosensing system and conventional method.

548 **Table 1.** Assessment of blood sugar content using GDH-GBP/Au based biosensing system and
549 conventional method.

Number of whole blood samples	**Glucose concentration measured by HK protocols (mM) (a)**	**Glucose concentration measured by GDH-GBP/Au based biosensor (mM) (b)**	**Relative deviation (%)[a]**
1	6.68±0.01	8.17±0.36	9.19
2	5.57±0.03	6.39±0.07	3.97
3	5.30±0.01	6.35±0.08	8.11
4	5.07±0.00	5.72±0.17	4.64
5	4.72±0.01	5.22±0.22	6.49

550 [a]Relative deviation (%) = 100×|b-a|/b (The average value was used for calculation of relative
551 deviation.)

Figure captions

Fig. 1. (A) CV profiles of a bare Au electrode, GDH/Au, 1st and 20th scans of GDH-GBP/Au in the presence of 100 mM glucose in a PBS buffer (100 mM, pH 7.0). (B) Dependence of the electron transfer of GDH-GBP/Au on the scan rate (100, 80, 60, 50, 40, 30, 20, and 10 mV s^{-1}) (inset: dependence of the peak current on root square of the scan rate).

Fig. 2. Gold binding characteristics of the native- and GBP-fused FAD-GDH. (A) Gold binding activities of the native- and GBP-fused FAD-GDH on a gold-coated quartz crystal, determined by measuring the frequency changes using quartz crystal microbalance (QCM) analysis. (B) AFM images showing the surface topographies of the native- and GBP-fused FAD-GDH system (protein concentration: 55 μg mL^{-1}). The areas correspond to 1 μm × 1 μm scans.

Fig. 3. (A) Dependence of the steady-state catalytic current at the GDH-GBP/Au on the 0 to 200 mM of glucose concentration. (Insert: Dotted trace represents the current response up to 10 mM of glucose concentration) Data fitted to the Michaelis-Menten equation by using non-linear regression analysis. (B) Schematic illustrations of the screen-printed electrode used here, the electrochemical characterization of the enzyme–electrode, and interfacial electron transfer of native- and GBP-fused FAD-GDH on surface of the screen-printed electrode (top inset: photograph of a bare screen-printed electrode).

Fig. 3. Amperometric response of GDH-GBP/Au toward sequential addition of (A) 10 mM of other type sugars (fructose, galactose, and xylose) and (B) 1 mM of reducing compounds (ascorbic acid, uric acid, and acetaminophen) in PBS solution after initial addition of 100 mM of glucose at an applied potential of -0.2 V (*vs.* Ag/AgCl).

Fig. 5. (A) Dependence of the steady-state catalytic current at the GDH-GBP/Au on the glucose concentration (0 to 200 mM) at different incubation temperatures (30, 40, and 50°C). Applied potential is -0.2 V (*vs.* Ag/AgCl) Data fitted to the Michaelis-Menten equation by using non-linear regression analysis. (B) Plot of K_M^{app} of GDH-GBP/Au obtained from the glucose concentration-dependent amperometric signals (green) and the specific activity of the free GBP-fused FAD-GDH of the electrolyte at 30, 40, 50°C (red).

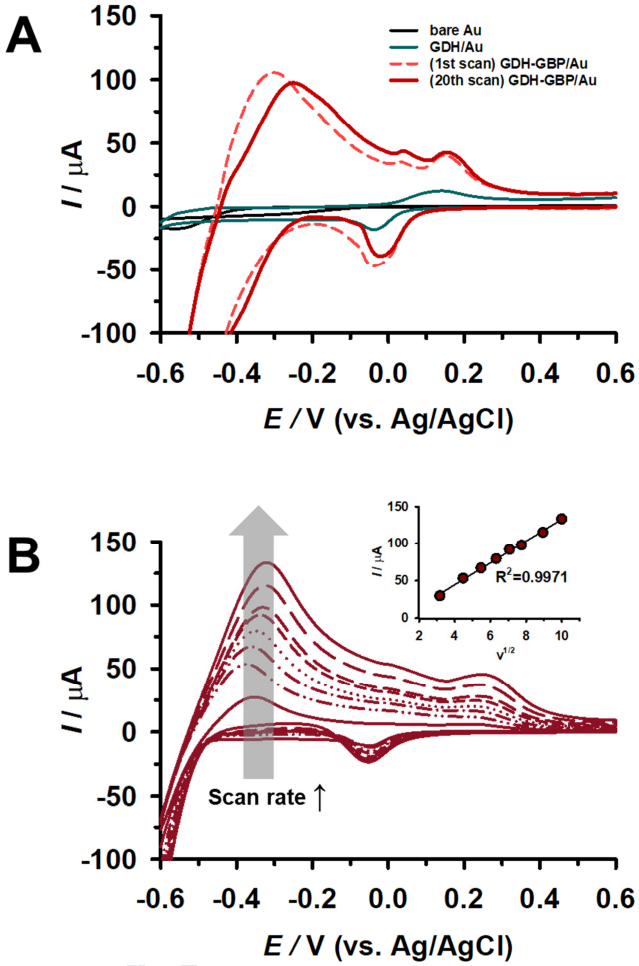

Fig. 1. (A) CV profiles of a bare Au electrode, GDH/Au, 1st and 20th scans of GDH-GBP/Au in the presence of 100 mM glucose in a PBS buffer (100 mM, pH 7.0). (B) Dependence of the electron transfer of GDH-GBP/Au on the scan rate (100, 80, 60, 50, 40, 30, 20, and 10 mV s^{-1}) (inset: dependence of the peak current on root square of the scan rate).

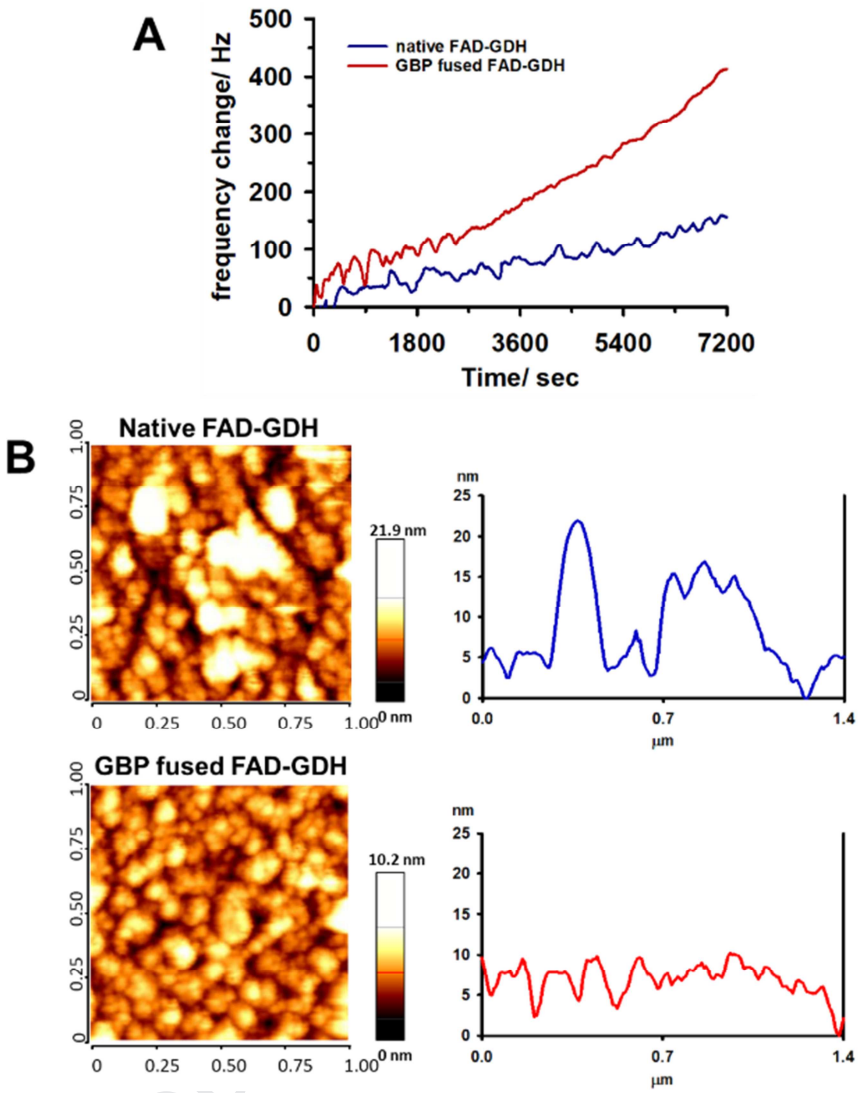

Fig. 2. Gold binding characteristics of the native- and GBP-fused FAD-GDH. (A) Gold binding activities of the native- and GBP-fused FAD-GDH on a gold-coated quartz crystal, determined by measuring the frequency changes using quartz crystal microbalance (QCM) analysis. (B) AFM images showing the surface topographies of the native- and GBP-fused FAD-GDH system (protein concentration: 55 μg mL^{-1}). The areas correspond to 1 μm × 1 μm scans.

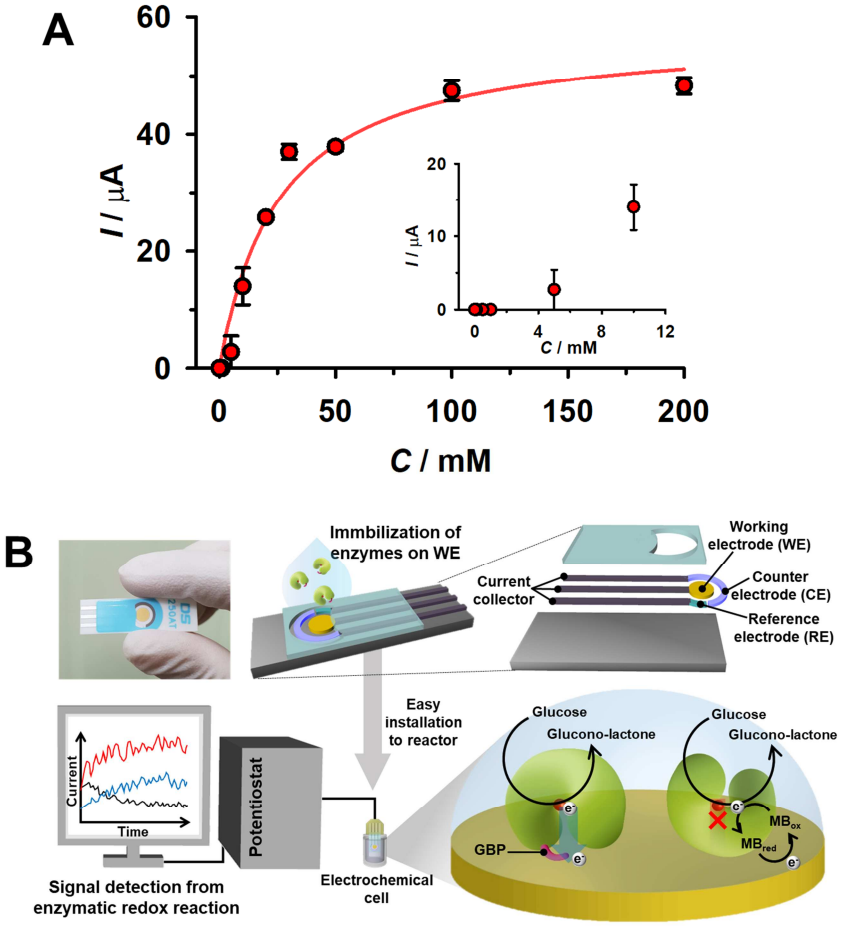

Fig. 3. (A) Dependence of the steady-state catalytic current at the GDH-GBP/Au on the 0 to 200 mM of glucose concentration. (Insert: Dotted trace represents the current response up to 10 mM of glucose concentration) Data fitted to the Michaelis-Menten equation by using non-linear regression analysis. (B) Schematic illustrations of the screen-printed electrode used here, the electrochemical characterization of the enzyme–electrode, and interfacial electron transfer of native- and GBP-fused FAD-GDH on surface of the screen-printed electrode (top inset: photograph of a bare screen-printed electrode).

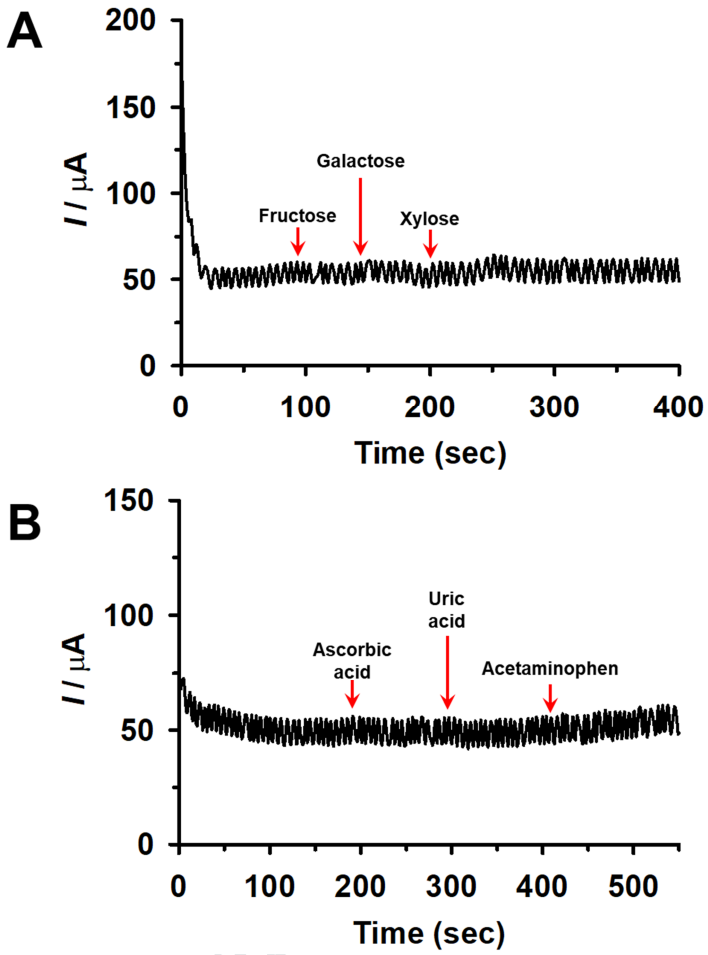

Fig. 4. Amperometric response of GDH-GBP/Au to sequential addition of (A) 10 mM of other type sugars (fructose, galactose, and xylose) and (B) 1 mM of reducing compounds (ascorbic acid, uric acid, and acetaminophen) in PBS solution after initial addition of 100 mM of glucose at an applied potential of -0.2 V (*vs.* Ag/AgCl)

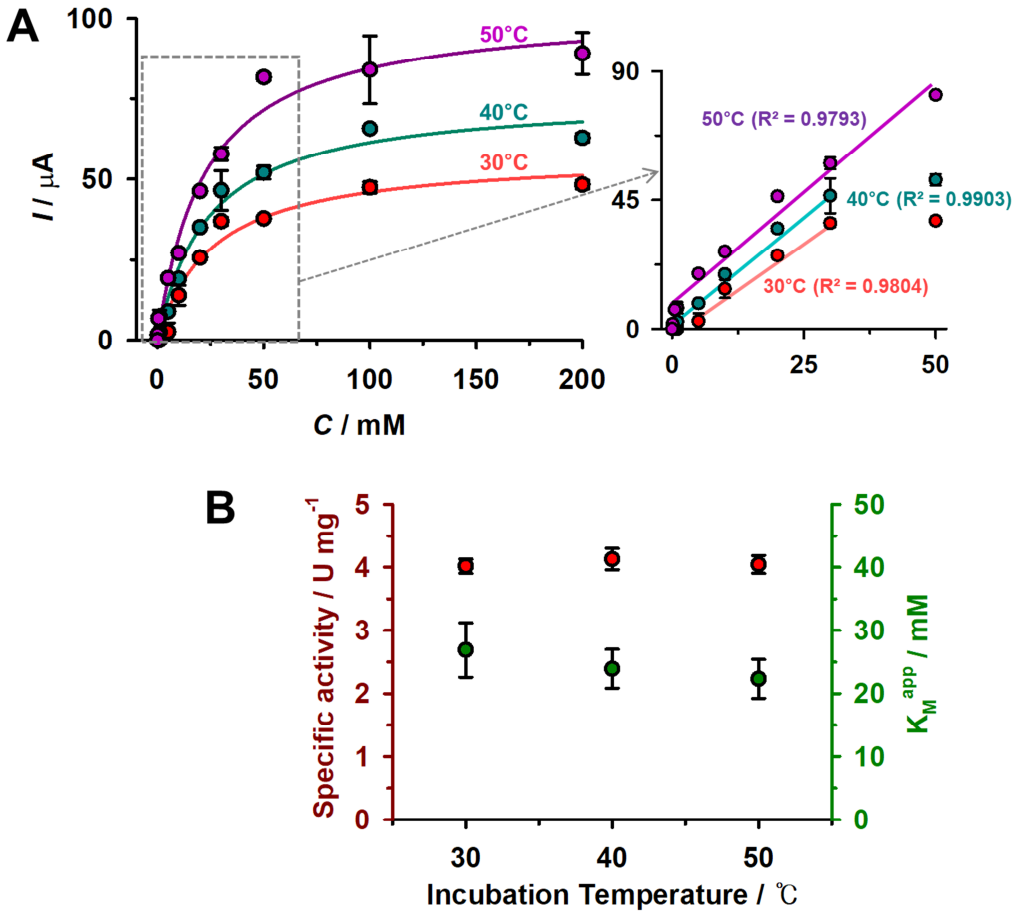

Fig. 5. (A) Dependence of the steady-state catalytic current at the GDH-GBP/Au on the glucose concentration (0 to 200 mM) at different incubation temperatures (30, 40, and 50°C). Applied potential is -0.2 V (*vs.* Ag/AgCl) Data fitted to the Michaelis-Menten equation by using non-linear regression analysis. (B) Plot of K_M^{app} of GDH-GBP/Au obtained from the glucose concentration-dependent amperometric signals (green) and the specific activity of the free GBP-fused FAD-GDH of the electrolyte at 30, 40, 50°C (red).

Research Highlights

- DET based biosensor was developed using GBP fused FAD-GDH on SPE.
- The fusion of GBP increased mechanical and electrical stability of FAD-GDH on SPE.
- The GDH-GBP/Au exhibits high selectivity toward glucose in whole human blood

Declaration of interests

☒ The authors declare that they have no known competing financial interests or personal relationships that could have appeared to influence the work reported in this paper.

☐The authors declare the following financial interests/personal relationships which may be considered as potential competing interests: